Progress in Natural Science: Materials International 26 (2016) 158–162

HOSTED BY

Contents lists available at ScienceDirect

Progress in Natural Science: Materials International

journal homepage: www.elsevier.com/locate/pnsmi

Improvements of dielectric properties of Cu doped $LaTiO_{3+\delta}$

Yan Chen [a,b,c], Jianxun Xu [a,b], Yimin Cui [b,*], Guangyi Shang [a,b], Jianqiang Qian [a,b], Jun-en Yao [a,b,c]

[a] Key Laboratory of Micro-nano Measurement-Manipulation and Physics, Ministry of Education, Beihang University, Beijing 100191, China
[b] School of Physics and Nuclear Energy Engineering, Beihang University, Beijing 100191, China
[c] School of Instrumentation Science and Opto-electronics Engineering, Beihang University, Beijing 100191, China

ARTICLE INFO

Article history:
Received 26 May 2015
Accepted 20 November 2015
Available online 21 April 2016

Keywords:
Cu doped $LaTiO_{3+\delta}$
Dielectric properties
Complex impedance

ABSTRACT

The ceramic composites of Cu-doped $La_{1-x}Cu_xTiO_{3+\delta}$ (x=0.05, 0.15, 0.3, 0.5) were synthesized by conventional solid-state reaction. The complex dielectric properties of the composites were investigated as a function of temperature (77 K ≤ T ≤ 320 K) and frequency (100 Hz ≤ f ≤ 1 MHz) separately. In all composites, the dielectric constants increase monotonously and the dielectric loss undulates with temperature. And it is clearly observed that extraordinarily high low-frequency dielectric constant (~10^4) appear at room temperature in $La_{0.5}Cu_{0.5}TiO_{3+\delta}$, which is ~100 times larger than that of $La_{0.95}Cu_{0.05}TiO_{3+\delta}$. Interestingly, the dielectric constants increase remarkably with the doped Cu contents, meanwhile the dielectric loss for all samples is ideal lower than 1 at room temperature in the measured frequency range. By means of complex impedance analysis, the improvements of dielectric properties are attributed to both bulk contribution and grain boundary effect, in which the bulk polaronic relaxation and the Maxwell–Wagner relaxation due to grain boundary response are heightened remarkably with the high doped Cu contents.

1. Introduction

$LaTiO_{3+\delta}$, according to the crystal structure, belongs to weakly distorted cubic perovskites [1–4]. In recent years, this compound has attracted increasing attention since they show a huge variety of exceptional features, such as high-temperature superconductivity, colossal magnetoresistance and metal insulator transition (MIT) [5–7]. $LaTiO_{3+\delta}$ is a prototypical Mott–Hubbard insulator, which is at the verge of a metal–insulator (MI) transition, becoming metallic at very low doping levels [8]. Lanthanum titanate oxide materials offer a large range of electronic properties depending on the oxygen amount δ. $LaTiO_{3.5}$, $LaTiO_{3+\delta}$, and $LaTiO_3$ thin films have shown to be insulating and ferroelectric, semiconductive, and metallic, respectively [9–12].

As one of the promising materials, $LaTiO_{3+\delta}$ has attracted much scientific attention [13–16]. Vilquin and colleagues [17] demonstrated that resistivity and metallic properties of $LaTiO_3$ were influenced by doping with Sr. Ziani et al. [18] reported that oxygen and nitrogen content could affect the structural and dielectric properties. Schmehl's group [19] studied the transport properties of $LaTiO_{3+\delta}$. Zhang et al. [20] found that B-site Cu-doped $LaTiO_3$ showed highly fenton activity and stability for the degradation of RHB with H_2O_2 in the initial pH range of 4–9.

In our earlier work [21], we reported that the dielectric constants of oxygen-doped polycrystalline La_2CuO_{4+y}, which exhibited the coexistence of superconducting and antiferromagnetic phases, were substantially larger than all previously reported values in La-based cuprates. Up to now, there has been no report about the dielectric properties of A-site Cu-doped $LaTiO_{3+\delta}$. In this paper, $La_{1-x}Cu_xTiO_{3+\delta}$ (x=0.05, 0.1, 0.3, and 0.5) are prepared by conventional solid state reaction and the complex dielectric properties of the samples are discussed thoroughly as the function of temperature (77 K ≤ T ≤ 320 K) and frequency (100 Hz ≤ f ≤ 1 MHz), respectively.

2. Experimental

A set of ceramic Cu-doped samples were prepared by a solid state reaction method. Firstly, the stoichiometric amounts of La_2O_3, CuO, and TiO_2 powders with high purity (99.99%) were mixed and grinded in an agate mortar for about 1 h approximately. And then they were sintered at 1100 °C for 600 min. The grinding and sintering processes were repeated for three times. Finally, the obtained powders were reground and pressed into disks with

* Corresponding.
E-mail address: cuiym@buaa.edu.cn (Y. Cui).
Peer review under responsibility of Chinese Materials Research Society.

http://dx.doi.org/10.1016/j.pnsc.2016.03.001

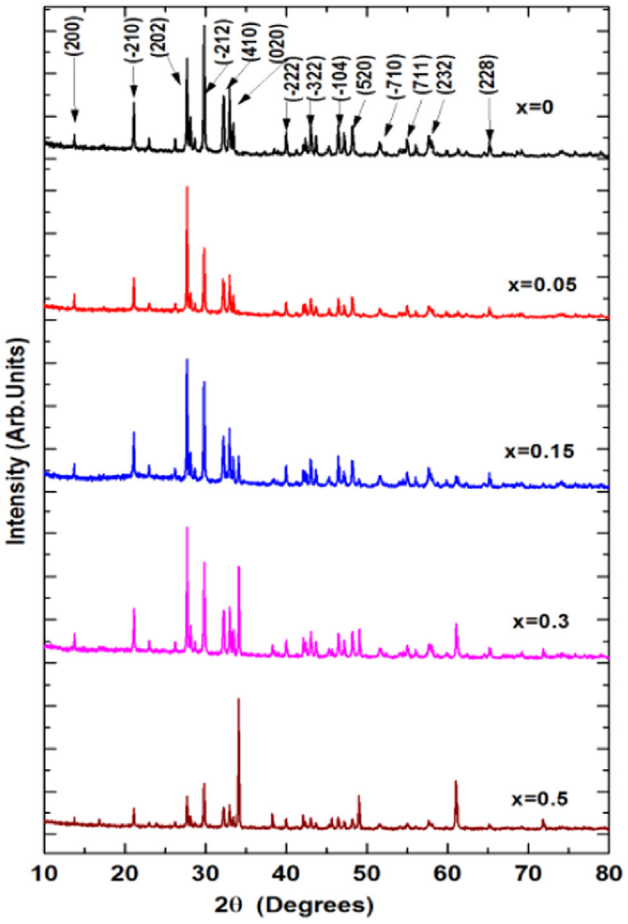

Fig. 1. The XRD patterns for $La_{1-x}Cu_xTiO_{3+\delta}$ (x=0, 0.05, 0.15, 0.3, and 0.5) at room temperature.

7.0 mm in diameter and 1.6 mm in thickness. The disks were sintered at 1150 °C in air for another 600 min, and then cooled down to room temperature with furnace.

The samples were characterized by X-ray diffraction (XRD) at room temperature using X'Pert PRO (Panalytical B.V, Netherlands). Surface morphologies of bulks were measured by scanning electron microscopy (SEM, model: S-4800). Electrodes were prepared by coating silver paste on both sides of the disk-type samples. The temperature dependent dielectric properties (capacitance and dielectric loss) were measured using the Quadtech ZM2353 LCR digibridge in a frequency range of 100 Hz–200 kHz. The frequency dependent dielectric properties and complex impedance were tested with a precision impedance analyzer 6500B (Wayne kerr corp.) in a frequency range of 100 Hz–1 MHz at different temperatures [22–25].

3. Results and discussion

The X-ray diffraction patterns of as-prepared samples at room temperature are shown in Fig. 1. The four Cu-doped samples are nearly single phases which are almost the same as the parent $LaTiO_{3+\delta}$ sample. However, the intensities of the peaks change gradually with the increase of concentration of doped copper separately. It is clearly seen that the peak intensities of $La_{0.5}Cu_{0.5}TiO_{3+\delta}$ sample are more different from other samples, and the perovskite structure may be destroyed by heavily doping of Cu cations. It also can be seen that a few small impurity peaks

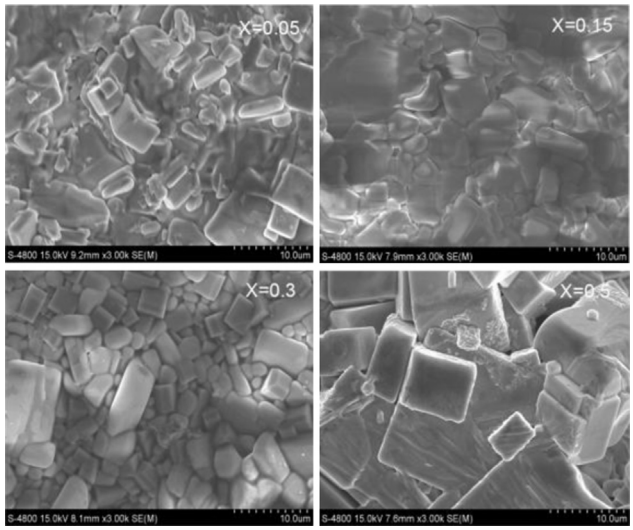

Fig. 2. The typical scanning electron micrographs of the $La_{1-x}Cu_xTiO_{3+\delta}$ (x=0.05, 0.15, 0.3, and 0.5) samples.

are showed in the X-ray data, which could be attributed to phase contributions emanating from a small degree of unintended non-stoichiometry. In fact, a small amount of copper oxide may be produced and mixed in the as-prepared samples.

The typical scanning electron micrographs are illustrated in Fig. 2. The ceramic samples are cubical or rectangle grains, with several micrometers in size. It is obvious that the grains of $La_{0.5}Cu_{0.5}TiO_{3+\delta}$ are the biggest among the four samples. Although these samples were prepared using the same pressure and sintering time, it is clearly observed that the consistency of grains becomes better with the increase of copper concentration.

Fig. 3(a), (c), (e) and (g) shows the typical results of the variation in dielectric constant $\varepsilon'(T)$ and dielectric loss tangent $\tan\delta(T)$ with the temperature for the four Cu-doped samples. Dielectric constants are given by the following equation [24]:

$$\varepsilon' = \frac{Cd}{S\varepsilon_0} \tag{1}$$

In which, C is the capacitance between the two plates, d is the thickness of the sample, S is the area of the round face painted with silver plate, and ε_0 is the permittivity of vacuum. It can be seen that all the dielectric constants $\varepsilon'(T)$ increase monotonously with temperature which shows obvious reversed frequency dependence. Interestingly, the dielectric constants increase remarkably with the doped Cu contents. It is clearly observed that extraordinarily high low-frequency dielectric constants ($\sim 10^4$) appear at room temperature in $La_{0.5}Cu_{0.5}TiO_{3+\delta}$ sample, while that of $La_{0.95}Cu_{0.05}TiO_{3+\delta}$, $La_{0.85}Cu_{0.15}TiO_{3+\delta}$, $La_{0.7}Cu_{0.3}TiO_{3+\delta}$ samples are no more than 140, 500, 5000, respectively. The curves of $La_{0.95}Cu_{0.05}TiO_{3+\delta}$ exhibit two $\varepsilon'(T)$ plateaus that appeared at low and high temperatures. Between the two plateaus, the curves increase rapidly in $\varepsilon'(T)$ with the increasing of the temperature. And all the other ceramic samples have one plateau at low temperature which increases rapidly with temperature at high temperature range. The above facts indicate that there exist two thermally activated dielectric relaxations in the four samples. For brevity, the low- and high-temperature relaxations are labeled as LTR and HTR, respectively.

Fig. 3(b), (d), (f) and (h) shows the temperature dependence of the dielectric loss tangent $\tan\delta(T)$. For the four samples, obvious peaks (or kinks) exist in the curves, which correspond to the sharp changes in $\varepsilon'(T)$ mentioned above. A close inspection reveals that,

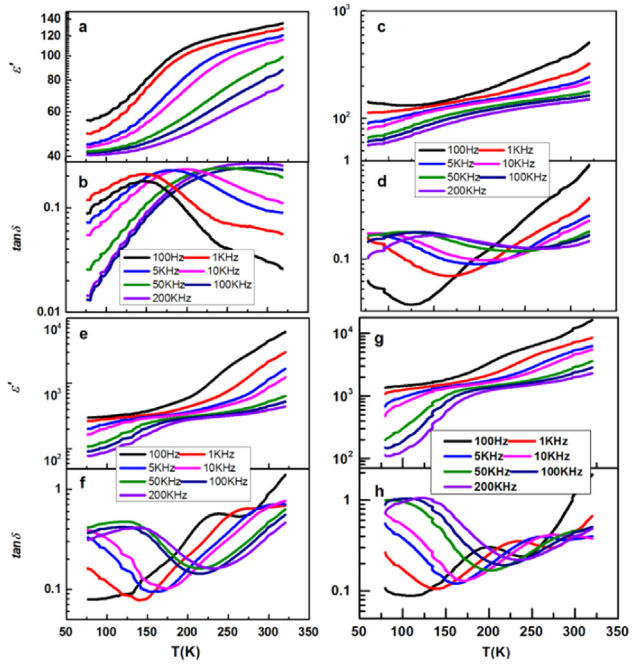

Fig. 3. The temperature dependence of the dielectric constant $\varepsilon'(T)$ ((a), (c), (e), and (g)) and the dielectric loss tangent $\tan\delta(T)$ ((b), (d), (f) and (h)) of the $La_{0.95}Cu_{0.05}TiO_{3+\delta}$, $La_{0.85}Cu_{0.15}TiO_{3+\delta}$, $La_{0.7}Cu_{0.3}TiO_{3+\delta}$, and $La_{0.5}Cu_{0.5}TiO_{3+\delta}$ samples, the frequency range is 100 Hz–200 KHz.

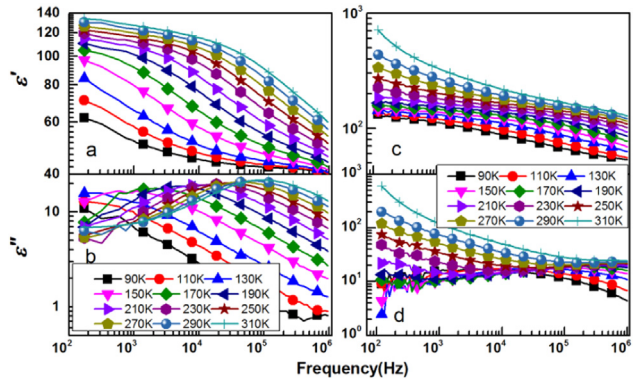

Fig. 4. The frequency dependence of the dielectric constant $\varepsilon'(T)$ ((a), (c)) and the imaginary dielectric constant $\varepsilon''(T)$ ((b), (d)) of the $La_{0.95}Cu_{0.05}TiO_{3+\delta}$, $La_{0.85}Cu_{0.15}TiO_{3+\delta}$ samples, the temperature range is 90–310 K.

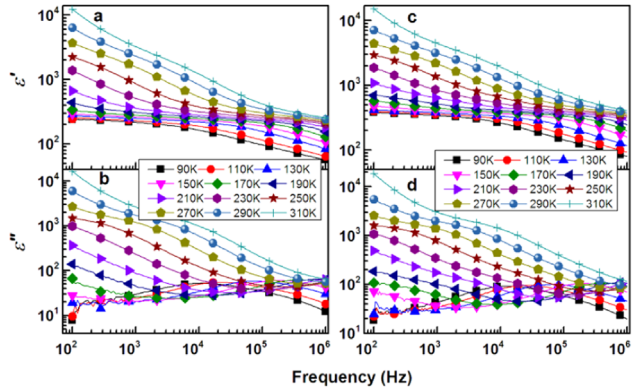

Fig. 5. The frequency dependence of the dielectric constant $\varepsilon'(T)$ ((a), (c)) and the imaginary dielectric constant $\varepsilon''(T)$ ((b), (d)) of the $La_{0.7}Cu_{0.3}TiO_{3+\delta}$, and $La_{0.5}Cu_{0.5}TiO_{3+\delta}$ samples, the temperature range is 90–310 K.

besides the prominent peak in the loss tangent below 150 K, obvious peaks appear around 250 K in Fig. 3(f) and (h) respectively, and the corresponding dielectric constants exhibit a steep increase in Fig. 3(e) and (g) separately. These suggest that a new and strong relaxation process occurs in $La_{0.7}Cu_{0.3}TiO_{3+\delta}$, and $La_{0.5}Cu_{0.5}TiO_{3+\delta}$ samples respectively, which lead to the striking improvement of the dielectric constant. The dielectric loss of the samples increases slightly with the doped Cu contents. The values of their dielectric loss are ideally lower than 1 for all samples at room temperature in the measured frequency range. As the measured frequency increasing, the loss peak positions move to high temperature, which shows a thermally excited relaxation process. Because of Cu doping, the conductivity and polarization of the samples may be change of to some degree, which jointly determine the dielectric loss. As a result, the dielectric loss for all samples is different one another.

Figs. 4 and 5 show the log–log plots of $\varepsilon'(T)$ and $\varepsilon''(T)$ versus frequency of the four Cu-doped samples sequentially at the fixed temperature, where $\varepsilon''(T) = \varepsilon'(T) \cdot \tan\delta(T)$. As shown in Figs. 4(a) and (c), and 5(a) and (c), in the condition of the higher temperature, most of the curves of the dielectric constants drop nonlinearly with the increasing frequency. The dielectric constants are strongly dependent on the temperature and the frequency, which is a clear signature of dielectric behavior being dictated by the regions of different conductivities. For the $La_{0.95}Cu_{0.05}TiO_{3+\delta}$ sample the $\varepsilon'(T)$decreases more quickly at higher frequencies, especially in the higher temperature. For the heavily Cu doped samples, it is clearly observed that extraordinarily high low-frequency dielectric constants appear at room temperature in $La_{0.5}Cu_{0.5}TiO_{3+\delta}$ ($\varepsilon'(T) > 10^4$), which is ~100 times larger than that of $La_{0.95}Cu_{0.05}TiO_{3+\delta}$ ($\varepsilon'(T) \approx 140$). Shown in Fig. 5(a) and (c), the curves of $\varepsilon'(T)$ are declined more quickly at the higher temperature. The frequency dependency of $\varepsilon''(T)$ are shown in Figs. 4 (b) and (d), and 5(b) and (d). For the $La_{0.95}Cu_{0.05}TiO_{3+\delta}$ sample, a group of obvious peaks exists in the curves of Fig. 4(b), which correspond to the sharp changes in $\varepsilon'(T)$ and move to higher frequencies with the temperature.

Obviously, for the heavily Cu doped samples, a group of obvious peaks are found in the lower temperature curves of Figs. 4(d) and, 5(b) and (d). At the same time, the higher temperature curves demonstrate that most of the experimental data fall on a straight line in the covered frequency range, indicating that the conductivity has overwhelming contribution to energy dissipation. However, the several data points of $\varepsilon'(T)$ deviate from the straight line at the lower temperature and higher frequency, which shows that localized polarization charge carrier have contribution to $\varepsilon''(T)$ except for the conductivity. It is known that the condensation of the polarized clusters are more easily emerges at low temperature relatively and their domain walls cause an obvious delay of the response to the external alternating field at higher frequency.

Fig. 6(a)–(d) shows complex impedance spectrums of the four Cu-doped samples measured at 270 K. The impedance spectrum is characterized by the appearance of semicircular arcs, whose pattern of evolution changes with temperature. The Z′ and Z″are the real and imaginary parts of electrical impedance, respectively. By fitting, two semicircular arcs can be sketched in impedance patterns of the four samples in Fig. 6. The analysis of the curves shows that those semicircles all exhibit some depression degree instead of semicircles centered on the real axis. This decentralization obeys the Cole–Cole's formalism, which is given by the following equation:

$$Z^*(\omega) = \frac{R}{1 + (j\omega/\omega_0)^{1-n}} \quad (2)$$

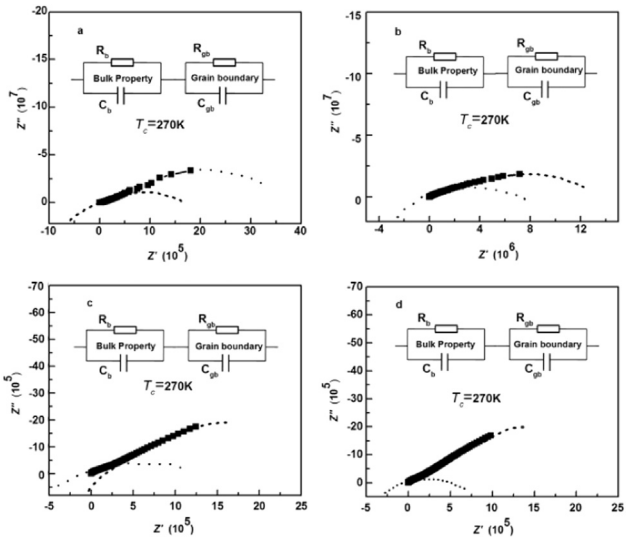

Fig. 6. Complex impedance spectrums of (a) $La_{0.95}Cu_{0.05}TiO_{3+\delta}$, (b) $La_{0.85}Cu_{0.15}TiO_{3+\delta}$, (c) $La_{0.7}Cu_{0.3}TiO_{3+\delta}$, and (d) $La_{0.5}Cu_{0.5}TiO_{3+\delta}$ at measured temperature 270 K.

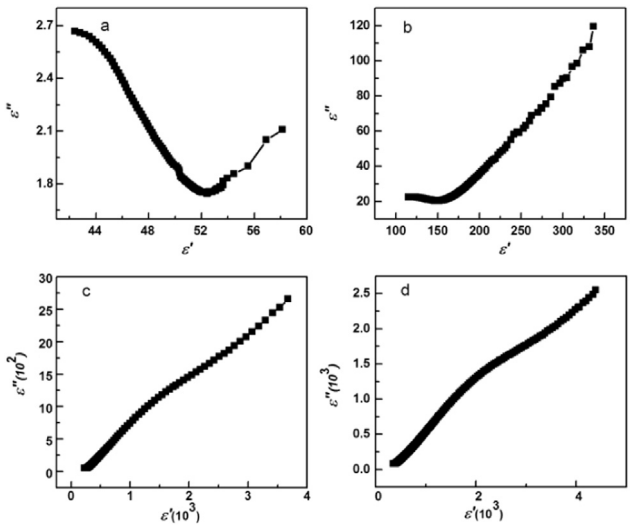

Fig. 7. Nyquist plots (ε''–ε') of (a) $La_{0.95}Cu_{0.05}TiO_{3+\delta}$, (b) $La_{0.85}Cu_{0.15}TiO_{3+\delta}$, (c) $La_{0.7}Cu_{0.3}TiO_{3+\delta}$, and (d) $La_{0.5}Cu_{0.5}TiO_{3+\delta}$ at measured temperature 270 K.

where the depressed semicircle represents a typically phenomenon with a distribution of relaxation time for $n < 1.00$. The relaxation distribution phenomenon has been reported for ceramic with perovskite structures [24]. The presence of two semicircular arcs in impedance patterns in Fig.6 illustrates that electrical processes in the compounds take place with definite contributions from both bulk (grain interior) and grain boundary effects, which can approximately be modeled by a combination of two parallel R–C circuits (insets of Fig. 6).

Fig. 7(a)–(d) shows Nyquist plots (ε''–ε') of the four Cu-doped samples at 270 K separately. According to impedance spectrums, there are obvious inflexions which also can be fit to two semicircular. The unsymmetrical profiles of ε'' indicate the two times relaxation in the four samples, in which the electrical relaxations may not be inappropriate described by the Debye equation. For the four ceramic samples, the loss tangent $\tan\delta(T)$ peaks shift to higher temperature with increasing frequency, which indicates that the dielectric behaviors mainly originate from the thermally activated relaxation process [26,27]. For a thermally activated relaxation process, the temperature dependence of the relaxation time follows the Arrhenius law:

$$\tau = \tau_0 \exp(U/K_B T) \tag{3}$$

where K_B is the Boltzmann constant, which value is 8.617343×10^{-5} eV/K and τ_0 is the relaxation time at infinite temperature, and U denotes the activation energy required for the relaxation. The Arrhenius plot of the relaxation rate, obtained from the dielectric loss tangent $\tan\delta(T)$, as a function of inverse temperature are shown in Figs. 8 and 9. Linear change of $\ln\tau$ versus $1/T$ describes the data quite well, as indicated by the solid lines. For LTR, according to Fig. 8(a)–(d), the activation energy U was found as 0.07 eV, 0.031 eV, 0.052 eV and 0.013 eV for the Cu-doped $La_{1-x}Cu_xTiO_{3+\delta}$ (x=0.05, 0.15, 0.3, and 0.5) samples, respectively. And as for HTR, from Fig. 9(a) and (b), the activation energy U was found to be 0.148 eV and 0.127 eV for the Cu-doped $La_{1-x}Cu_xTiO_{3+\delta}$ (x=0.3, and 0.5) samples, which are higher than that in LTR. These experimental results imply that the nature of charge carries is responsible for dielectric relaxation peaks and dc conduction which belongs to same category.

We now turn our attention to the origin of the LTR and HTR relaxations. From the dielectric loss tangent in Fig. 3, it is clearly seen that the peak height of LTR gradually increases as the peak

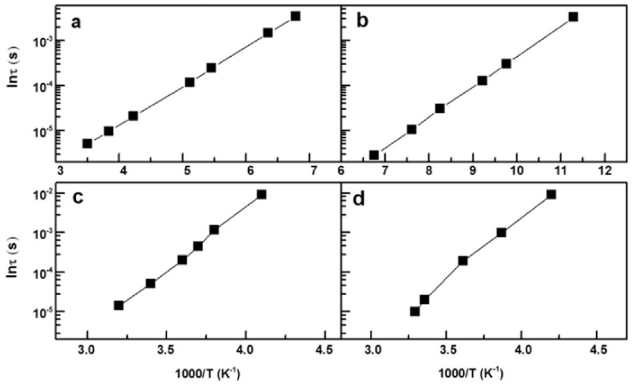

Fig. 8. The Arrhenius plots (a), (b), (c) and (d) of the relaxation time for LTR, as a function of inverse temperature from $\tan\delta(T)$ maximum for the polycrystalline $La_{0.95}Cu_{0.05}TiO_{3+\delta}$, $La_{0.85}Cu_{0.15}TiO_{3+\delta}$, $La_{0.7}Cu_{0.3}TiO_{3+\delta}$, and $La_{0.5}Cu_{0.5}TiO_{3+\delta}$ samples.

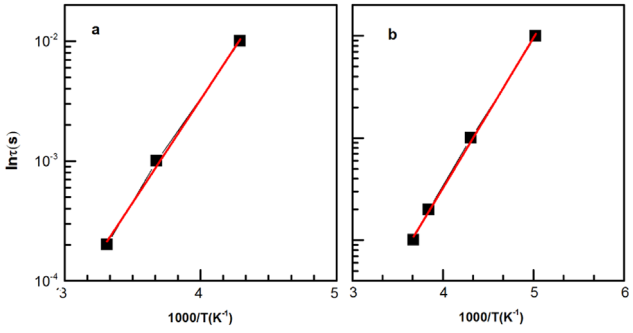

Fig. 9. The Arrhenius plots (a) and (b) of the relaxation time for HTR, as a function of inverse temperature from $\tan\delta(T)$ maximum for the polycrystalline $La_{0.7}Cu_{0.3}TiO_{3+\delta}$ and $La_{0.5}Cu_{0.5}TiO_{3+\delta}$ samples.

position shifts to higher temperatures with increasing frequencies. This fact implies that the LTR might be related to a polaronic relaxation as reported in Ga doped $LaFeO_3$ [28], which increase with the doped content. As for the HTR in the $La_{0.7}Cu_{0.3}TiO_{3+\delta}$, and $La_{0.5}Cu_{0.5}TiO_{3+\delta}$ samples, the Cu content is so high that the Cu particles may accumulate at the grain boundary, which leads to inhomogeneous Cu distribution in the composites. At the same

time, the inhomogeneity of oxygen distribution may also exist at grain boundary. These inhomogeneous distributions contribute to the large difference in the conductivity. Hence, at 250 K it is strongly indicative of a Maxwell–Wagner type relaxation, associated with an inhomogeneous dielectric medium containing two or more layers of materials with different permittivity and conductivity. An external electric field, inducing an electric current along the material, produces a charge carrier concentration discontinuity across the interface between more and less conductive regions. The build-up of charge results in the Maxwell–Wagner type relaxation [29,30].

4. Conclusion

In summary, polycrystalline Cu-doped ceramic samples were fabricated by conventional solid-state reaction. Investigations on dielectric properties of the ceramic samples have been performed. And it is clearly observed that the higher low-frequency dielectric constant appear at room temperature in $La_{0.5}Cu_{0.5}TiO_{3+\delta}$=, which is ~100 times larger than that of $La_{0.95}Cu_{0.05}TiO_{3+\delta}$. Interestingly, Complex impedance analysis reveals that electrical processes of different samples can be attributed to the combined actions of bulk polaronic properties and grain boundary effects.

Acknowledgment

We acknowledge the financial support from National Natural Science Foundation of China (Nos. 51331002 and 51571006).

References

[1] A.A. Mozhegorov, A.E. Nikiforov, A.V. Larin, A.V. Efremov, L.É. Gonchar, P. A. Agzamova, Phys. Solid State 50 (2008) 1795.
[2] M. Bradha, S. Hussain, S. Chakravarty, G. Amarendra, A. Ashok, J. Alloy. Compd. 626 (2014) 245.
[3] B. Keimer, D. Casa, A. Ivanova, J.W. Lynn, M. Zimmermann, J.P. Hill, D. Gibbs, Y. Taquchi, Y. Tokura, Phys. Rev. Lett. 85 (2000) 3946.
[4] S. Okatov, A. Poteryaev, A. Lichtenstein, Eurphys. Lett. 70 (2005) 499.
[5] M. Imada, A. Fujimori, Y. Tokura, Rev. Mod. Phys. 70 (1998) 1039.
[6] J. Biscaras, N. Berqeal, A. Kushwaha, T. Wolf, A. Rastoqi, R.C. Budhani, J. Lesueur, Nat. Commun. 89 (2010) 1038.
[7] C. Ulrich, A. Gossling, M. Gruninger, M. Guennou, H. Roth, M. Cwik, T. Lorenz, G. Khaliullin, B. Keimer, Phys. Rev. Lett. 97 (2006) 157401.
[8] L. Craco, M.S. Laad, S. Leoni, E. Muller-Hartmann, Phys. Rev. B 70 (2003) 195116.
[9] I.V. Soloxyev, Phys. Rev. B 69 (2004) 134403.
[10] S. Okamoto, A.J. Millis, N.A. Spaldin, Phys. Rev. Lett. 97 (2006) 056802.
[11] F. Lichtenberg, D. Widmer, J.G. Bednorz, T. Williams, A. Relier, Phys. B: Condens. Matter 82 (1991) 211.
[12] A. Schmehl, F. Lichtenberg, H. Bielefeldt, J. Mannhart, Appl. Phys. Lett. 82 (2003) 3077.
[13] P. Lunkenheimer, T. Rudolf, J. Hemberger, A. Pimenov, S. Tachos, F. Lichtenberg, A. Loidl, Phys. Rev. B 68 (2003) 245108.
[14] M. Bradha, S. Hussain, S. Chakravarty, G. Amarendra, A. Ashok, Ionics 20 (2014) 1343.
[15] J. Fompeyrine, J.W. Seo, J.P. Locquet, Ceram. Soc. 19 (1999) 1493.
[16] T.A. Tyson, T. Wu, K.H. Ahn, S.B. Kim, S.W. Cheong, Phys. Rev. B 81 (2010) 054101.
[17] B. Vilquin, T. Kanki, T. Yanagida, H. Tanaka, Solid State Commun. 136 (2005) 328.
[18] A. Ziani, C.L. Paven-Thivet, L.L. Gendre, D. Fasquelle, J.C. Carru, F. Tessier, J. Pinel, Thin Solid Films 517 (2008) 544.
[19] A. Schmehl, F. Lichtenberg, H. Bielefeldt, J. Mannhart, D.G. Scholm, Appl. Phys. Lett. 82 (2003) 3077.
[20] L.L. Zhang, Y.L. Nie, C. Hu, J.H. Qu, Appl. Catal. B: Environ. 125 (2012) 418.
[21] C.C. Wang, Y.M. Cui, G.L. Xie, C.P. Chen, L.W. Zhang, Phys. Rev. B 72 (2005) 064513.
[22] J.X. Xu, Y.M. Cui, H.Z. Xu, Ceram. Int. 40 (2014) 12193.
[23] C. Lu, Y.M. Cui, Physica B 432 (2014) 58.
[24] C. Lu, Y.M. Cui, Physica B 407 (2012) 3856.
[25] J.X. Xu, Y.M. Cui, Mater. Sci. Eng. B 178 (2013) 316.
[26] Y.M. Cui, L.W. Zhang, C.L. Xie, R.M. Wang, Solid State Commun. 138 (2006) 481.
[27] Y.M. Cui, L.W. Zhang, R.M. Wang, Physica C 442 (2006) 29.
[28] S. Komine, E. Iguchi, J. Phys. Chem. Solids 68 (2007) 1504.
[29] C.C. Wang, Y.J. Yan, L.W. Zhang, Y.M. Cui, G.L. Xie, B.S. Cao, Scr. Mater. 54 (2006) 1501–1504.
[30] Q.J. Li, S.Q. Xia, X.,Y. Wang, W. Xia, Y. Yu, Y.M. Cui, J. Zhang, J. Zheng, C. Cheng, Y.D. Li, H. Wang, S.G. Huang, C.C. Wang, J. Alloy. Compd. 616 (2014) 577–580.